FACTA UNIVERSITATIS
Series: **Electronics and Energetics** Vol. 26, N° 2, August 2013, pp. 133 - 143
DOI: 10.2298/FUEE1302133P

SHAPE OF IMPULSE RESPONSE CHARACTERISTICS OF LINEAR-PHASE NONRECURSIVE 2D FIR FILTER FUNCTION*

Vlastimir D. Pavlović, Dejan N. Milić, Jelena R. Djordjević-Kozarov

University of Niš, Faculty of Electronic Engineering, Serbia

Abstract. *An analytical method for the new class of linear-phase multiplierless 2D FIR filter functions generated by applying the Christoffel-Darboux formula for classical Chebyshev polynomials of the first and the second kind, proposed in [6] was used for designing of linear-phase multiplierless 2D FIR filter described in this paper. Correct transformation from continuous two-dimensional domain into the z domains without residuum and without errors is described. The proposed solution high selectivity is a filter function in the z1 domain, and the Hilbert transformer in the z2 domain. The impulse response coefficients of proposed 2D FIR filter functions are presented in this paper, and corresponding examples of impulse response are illustrated. The paper also presents detailed analysis of the size of pass-band and stop-band of proposed multiplierless linear-phase 2D FIR filter function. Normalized surface area of the filter function pass-band is 3.45789156 10^{-5} for given maximal attenuation of 0.28 dB. Normalized surface area of the filter function stop-band is 80.395% for the given minimal attenuation of 100 dB.*

Key words: *2D FIR filter function, Multiplierless, Linear-phase, Impulse response characteristics, Coefficients of impulse response characteristic, Frequency response analysis, Diamond sharpness*

1. INTRODUCTION

The description and the proof of the extremal property of the Christoffel-Darboux sum for classical orthonormal polynomials for a given interval of orthogonality and a given weighting function are given in capital books [1, 2]. The application of the Christoffel-Darboux sum in the theory of filter functions for continuous 1D and 2D domain is given in the references [3 - 11].

Iterative methods and many efficient algorithms for the design of 2D filters are discussed in references [12-20]. In [12] the authors discuss the various approaches of designing 1D and 2D FIR filters using the theory of weighted Chebyshev approximations.

Received May 05, 2013
Corresponding author: Vlastimir Pavlović
University of Niš, Faculty of Electronic Engineering, Niš, Serbia
E-mail: vlastimir.pavlovic@elfak.ni.ac.rs
Acknowledgement: The paper is a part of the research done within the project No. 32023, funded by the Ministry of Science of the Republic of Serbia. The authors would like to thank to the Miodrag Popović, Faculty of Electrical Engineering, University of Belgrade, Serbia.

The different design and techniques are explained and compared. In [20] the method for circularly symmetric design of 2D wideband multiplierless FIR filter functions is given.

The 1D Hilbert transform in [21] has transfer function $e^{-j\pi/2}$ with asymmetric finite impulse response and has important applications in telecommunications.

This paper presents the further generalization of the previous research [5-7] in two dimensions. The proposed solution is a filter function in the *z1* domain, and the Hilbert transformer in the *z2* domain. An analytical method of the Christoffel-Darboux formula for the classical orthogonal Chebyshev polynomials, of the first and the second kind, is proposed in this paper in a compact explicit form in continuous domain. Also, the new class of the linear phase two-dimensional FIR digital filters, generated by the proposed modified formula and by direct mapping from the continuous domain into two-dimensional *z* domain, is given. The formula can be most directly applied for solving mathematically the approximation problem of a filter function of even and odd order. In order to illustrate, the examples of the efficient design of the new class of selective linear phase two-dimensional symmetric FIR digital filter functions are also given.

2. LINEAR-PHASE 2D FIR FILTER FUNCTION

Multiplierless linear-phase 2D FIR filter function with two free real parameters *K* and *M* is considered in this paper. A linear phase 2D FIR filter of $N\times N$-order is defined by

$$H(N,z_1,\ z_2)=K_1\sum_{r=0}^{N}\sum_{k=0}^{N}h(N,r,k)z_1^{-r}z_2^{-k} \tag{1}$$

where K_1 is the gain real constant and $h(N,r,k)$ are the filter coefficients that are real numbers. Squared filter magnitude response, in absolute units for $z_1\to e^{i\,\omega_1}$, $z_2\to e^{j\omega_2}$, can be presented as

$$\begin{aligned}H(\mathrm{N},z_1,\ z_2)H(\mathrm{N},\overline{z_1},\ \overline{z_2})&=\left|H(N,e^{i\omega_1},\ e^{j\omega_2})\right|^2=\\&=\left|H(N,e^{i\omega_1},\ e^{j\omega_2})\ H(N,e^{-i\omega_1},\ e^{-j\omega_2})\right|\end{aligned} \tag{2}$$

and

$$a(N,e^{i\omega_1},e^{j\omega_2})=10\log[H(N,e^{i\omega_1},e^{j\omega_2}]^2,\ \ \text{in}[dB] \tag{3}$$

If we directly apply the Christoffel-Darboux formula proposed in [6], a new class of 2D FIR filter functions can be obtained as

$$H(z_1,z_2)=-j\,K_1\sum_{r=1}^{N}(z_1^{+2r}+2+z_1^{-2r})\times(z_2^{+2r}-z_2^{-2r}) \tag{4}$$

Multiplying (4) with factor $z_1^{-2N}\cdot z_2^{-2N}$, the non-causal filter function becomes the causal filter function as

$$H(N,z_1,z_2)=-jK_1\cdot\sum_{r=1}^{N}[(z_1^{-2N+2r}+2\cdot z_1^{-2N}\cdot z_2^{-2N}+z_1^{-2N-2r})\times(z_2^{-2N+2r}-z_2^{-2N-2r})] \tag{5}$$

Evidently, from (4) is seen that the proposed FIR filter function is multiplierless, and has only adders. Thus, for even *N*, e.g. $N = 6$, we can see that the function $H(6,z_1,z_2)$ using (4) becomes

$$H(6,z_1,z_2)=1+z_1^{-24}+2\cdot z_1^{-12}-z_2^{-24}-z_1^{-24}z_2^{-24}-2\cdot z_1^{-12}z_2^{-24}-z_1^{-22}z_2^{-22}-2\cdot z_1^{-12}z_2^{-22}-z_1^{-2}z_2^{-22}-z_1^{-20}z_2^{-20}-2\cdot z_1^{-12}z_2^{-20}-z_1^{-4}z_2^{-20}-z_1^{-18}z_2^{-18}-2\cdot z_1^{-12}z_2^{-18}-z_1^{-6}z_2^{-18}-z_1^{-16}z_2^{-16}-2\cdot z_1^{-12}z_2^{-16}-z_1^{-8}z_2^{-16}-z_1^{-14}z_2^{-14}-2\cdot z_1^{-12}z_2^{-14}-z_1^{-10}z_2^{-14}+z_1^{-14}z_2^{-10}+2\cdot z_1^{-12}z_2^{-10}+z_1^{-10}z_2^{-10}+z_1^{-16}z_2^{-8}+2\cdot z_1^{-12}z_2^{-8}+z_1^{-8}z_2^{-8}+z_1^{-18}z_2^{-6}+2\cdot z_1^{-12}z_2^{-6}+z_1^{-6}z_2^{-6}+z_1^{-20}z_2^{-4}+2\cdot z_1^{-12}z_2^{-4}+z_1^{-4}z_2^{-4}+z_1^{-22}z_2^{-2}+2\cdot z_1^{-12}z_2^{-2}+z_1^{-2}z_2^{-2} \quad (6)$$

In the same way, for odd N, e.g. $N = 7$, we can see that the function $H(7,z_1,z_2)$ using (4) becomes

$$H(7,z_1,z_2)=1+z_1^{28}+2\cdot z_1^{-14}-z_2^{-28}-z_1^{-28}z_2^{-28}-2\cdot z_1^{-14}z_2^{-28}-z_1^{-26}z_2^{-26}-2\cdot z_1^{-14}z_2^{-26}-z_1^{-2}z_2^{-26}-z_1^{-24}z_2^{-24}-2\cdot z_1^{-14}z_2^{-24}-z_1^{-4}z_2^{-24}-z_1^{-22}z_2^{-22}-2\cdot z_1^{-14}z_2^{-22}-z_1^{-6}z_2^{-22}-z_1^{-20}z_2^{-20}-2\cdot z_1^{-14}z_2^{-20}-z_1^{-8}z_2^{-20}-z_1^{-18}z_2^{-18}-2\cdot z_1^{-14}z_2^{-18}-z_1^{-10}z_2^{-18}-z_1^{-16}z_2^{-16}-2\cdot z_1^{-14}z_2^{-16}-z_1^{-12}z_2^{-16}+z_1^{-16}z_2^{-12}+2\cdot z_1^{-14}z_2^{-12}+z_1^{-12}z_2^{-12}+z_1^{-18}z_2^{-10}+2\cdot z_1^{-14}z_2^{-10}+z_1^{-10}z_2^{-10}+z_1^{-20}z_2^{-8}+2\cdot z_1^{-14}z_2^{-8}+z_1^{-8}z_2^{-8}+z_1^{-22}z_2^{-6}+2\cdot z_1^{-14}z_2^{-6}+z_1^{-6}z_2^{-6}+z_1^{-24}z_2^{-4}+2\cdot z_1^{-14}z_2^{-4}+z_1^{-4}z_2^{-4}+z_1^{-26}z_2^{-2}+2\cdot z_1^{-14}z_2^{-2}+z_1^{-2}z_2^{-2} \quad (7)$$

3. 2D FIR Filter Function Impulse Response Characteristics

The impulse response coefficients from Eq. (1), $h(N,r,k)$, of the proposed 2D FIR filter from Eq. (4) for N=6, are given in the following matrix.

$$h(6,r,k)=\begin{bmatrix}
1 & 0 & 0 & 0 & 0 & 0 & 0 & 0 & 0 & 0 & 0 & 0 & 0 & 0 & 0 & 0 & 0 & 0 & 0 & 0 & 0 & 0 & 0 & 0 & -1 \\
0 & 0 & 0 & 0 & 0 & 0 & 0 & 0 & 0 & 0 & 0 & 0 & 0 & 0 & 0 & 0 & 0 & 0 & 0 & 0 & 0 & 0 & 0 & 0 & 0 \\
0 & 0 & 1 & 0 & 0 & 0 & 0 & 0 & 0 & 0 & 0 & 0 & 0 & 0 & 0 & 0 & 0 & 0 & 0 & 0 & 0 & 0 & -1 & 0 & 0 \\
0 & 0 & 0 & 0 & 0 & 0 & 0 & 0 & 0 & 0 & 0 & 0 & 0 & 0 & 0 & 0 & 0 & 0 & 0 & 0 & 0 & 0 & 0 & 0 & 0 \\
0 & 0 & 0 & 0 & 1 & 0 & 0 & 0 & 0 & 0 & 0 & 0 & 0 & 0 & 0 & 0 & 0 & 0 & 0 & 0 & -1 & 0 & 0 & 0 & 0 \\
0 & 0 & 0 & 0 & 0 & 0 & 0 & 0 & 0 & 0 & 0 & 0 & 0 & 0 & 0 & 0 & 0 & 0 & 0 & 0 & 0 & 0 & 0 & 0 & 0 \\
0 & 0 & 0 & 0 & 0 & 0 & 1 & 0 & 0 & 0 & 0 & 0 & 0 & 0 & 0 & 0 & 0 & 0 & -1 & 0 & 0 & 0 & 0 & 0 & 0 \\
0 & 0 & 0 & 0 & 0 & 0 & 0 & 0 & 0 & 0 & 0 & 0 & 0 & 0 & 0 & 0 & 0 & 0 & 0 & 0 & 0 & 0 & 0 & 0 & 0 \\
0 & 0 & 0 & 0 & 0 & 0 & 0 & 0 & 1 & 0 & 0 & 0 & 0 & 0 & 0 & 0 & -1 & 0 & 0 & 0 & 0 & 0 & 0 & 0 & 0 \\
0 & 0 & 0 & 0 & 0 & 0 & 0 & 0 & 0 & 0 & 0 & 0 & 0 & 0 & 0 & 0 & 0 & 0 & 0 & 0 & 0 & 0 & 0 & 0 & 0 \\
0 & 0 & 0 & 0 & 0 & 0 & 0 & 0 & 0 & 0 & 1 & 0 & 0 & 0 & -1 & 0 & 0 & 0 & 0 & 0 & 0 & 0 & 0 & 0 & 0 \\
0 & 0 & 0 & 0 & 0 & 0 & 0 & 0 & 0 & 0 & 0 & 0 & 0 & 0 & 0 & 0 & 0 & 0 & 0 & 0 & 0 & 0 & 0 & 0 & 0 \\
2 & 0 & 2 & 0 & 2 & 0 & 2 & 0 & 2 & 0 & 2 & 0 & 0 & 0 & -2 & 0 & -2 & 0 & -2 & 0 & -2 & 0 & -2 & 0 & -2 \\
0 & 0 & 0 & 0 & 0 & 0 & 0 & 0 & 0 & 0 & 0 & 0 & 0 & 0 & 0 & 0 & 0 & 0 & 0 & 0 & 0 & 0 & 0 & 0 & 0 \\
0 & 0 & 0 & 0 & 0 & 0 & 0 & 0 & 0 & 0 & 1 & 0 & 0 & 0 & -1 & 0 & 0 & 0 & 0 & 0 & 0 & 0 & 0 & 0 & 0 \\
0 & 0 & 0 & 0 & 0 & 0 & 0 & 0 & 0 & 0 & 0 & 0 & 0 & 0 & 0 & 0 & 0 & 0 & 0 & 0 & 0 & 0 & 0 & 0 & 0 \\
0 & 0 & 0 & 0 & 0 & 0 & 0 & 0 & 1 & 0 & 0 & 0 & 0 & 0 & 0 & 0 & -1 & 0 & 0 & 0 & 0 & 0 & 0 & 0 & 0 \\
0 & 0 & 0 & 0 & 0 & 0 & 0 & 0 & 0 & 0 & 0 & 0 & 0 & 0 & 0 & 0 & 0 & 0 & 0 & 0 & 0 & 0 & 0 & 0 & 0 \\
0 & 0 & 0 & 0 & 0 & 0 & 1 & 0 & 0 & 0 & 0 & 0 & 0 & 0 & 0 & 0 & 0 & 0 & -1 & 0 & 0 & 0 & 0 & 0 & 0 \\
0 & 0 & 0 & 0 & 0 & 0 & 0 & 0 & 0 & 0 & 0 & 0 & 0 & 0 & 0 & 0 & 0 & 0 & 0 & 0 & 0 & 0 & 0 & 0 & 0 \\
0 & 0 & 0 & 0 & 1 & 0 & 0 & 0 & 0 & 0 & 0 & 0 & 0 & 0 & 0 & 0 & 0 & 0 & 0 & 0 & -1 & 0 & 0 & 0 & 0 \\
0 & 0 & 0 & 0 & 0 & 0 & 0 & 0 & 0 & 0 & 0 & 0 & 0 & 0 & 0 & 0 & 0 & 0 & 0 & 0 & 0 & 0 & 0 & 0 & 0 \\
0 & 0 & 1 & 0 & 0 & 0 & 0 & 0 & 0 & 0 & 0 & 0 & 0 & 0 & 0 & 0 & 0 & 0 & 0 & 0 & 0 & 0 & -1 & 0 & 0 \\
0 & 0 & 0 & 0 & 0 & 0 & 0 & 0 & 0 & 0 & 0 & 0 & 0 & 0 & 0 & 0 & 0 & 0 & 0 & 0 & 0 & 0 & 0 & 0 & 0 \\
1 & 0 & 0 & 0 & 0 & 0 & 0 & 0 & 0 & 0 & 0 & 0 & 0 & 0 & 0 & 0 & 0 & 0 & 0 & 0 & 0 & 0 & 0 & 0 & -1
\end{bmatrix} \quad (8)$$

The 3D plot and 2D contour plot of impulse response characteristic, $h(N,r,k)$, of the proposed 2D FIR filter from Eq. (4) for even N=6, are given in the Fig. 1 and Fig. 2, respectively.

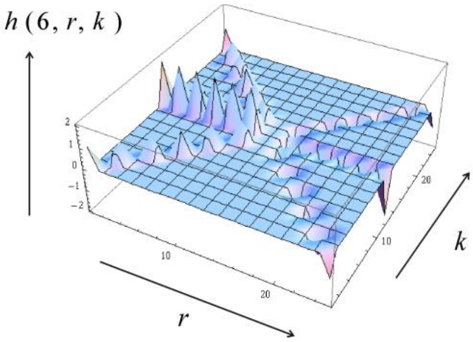

Fig. 1 3D plot of impulse response characteristic, $h(N,r,k)$, of the proposed 2D FIR filter from Eq. (4) for even N =6

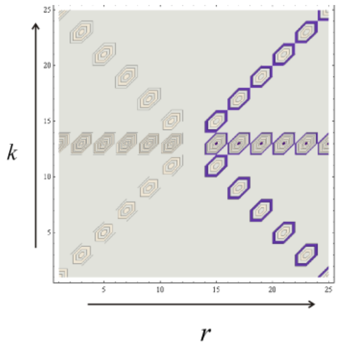

Fig. 2 2D contour plot of impulse response characteristic, $h(N,r,k)$, of the proposed 2D FIR filter from Eq. (4) for even N =6

Thus, the impulse response coefficients, $h(N,r,k)$, of the proposed filter for odd N=7, are given in the following matrix.

$$h(7,r,k)=\begin{bmatrix}
1&0&0&0&0&0&0&0&0&0&0&0&0&0&0&0&0&0&0&0&0&0&0&0&0&0&0&0&-1\\
0&0&0&0&0&0&0&0&0&0&0&0&0&0&0&0&0&0&0&0&0&0&0&0&0&0&0&0&0\\
0&0&1&0&0&0&0&0&0&0&0&0&0&0&0&0&0&0&0&0&0&0&0&0&0&0&-1&0&0\\
0&0&0&0&0&0&0&0&0&0&0&0&0&0&0&0&0&0&0&0&0&0&0&0&0&0&0&0&0\\
0&0&0&0&1&0&0&0&0&0&0&0&0&0&0&0&0&-1&0&0&0&0&0&0&0&0&0&0&0\\
0&0&0&0&0&0&0&0&0&0&0&0&0&0&0&0&0&0&0&0&0&0&0&0&0&0&0&0&0\\
0&0&0&0&0&0&1&0&0&0&0&0&0&0&0&-1&0&0&0&0&0&0&0&0&0&0&0&0&0\\
0&0&0&0&0&0&0&0&0&0&0&0&0&0&0&0&0&0&0&0&0&0&0&0&0&0&0&0&0\\
0&0&0&0&0&0&0&0&1&0&0&0&0&0&0&0&0&0&0&0&-1&0&0&0&0&0&0&0&0\\
0&0&0&0&0&0&0&0&0&0&0&0&0&0&0&0&0&0&0&0&0&0&0&0&0&0&0&0&0\\
0&0&0&0&0&0&0&0&0&0&1&0&0&0&0&0&0&0&-1&0&0&0&0&0&0&0&0&0&0\\
0&0&0&0&0&0&0&0&0&0&0&0&0&0&0&0&0&0&0&0&0&0&0&0&0&0&0&0&0\\
0&0&0&0&0&0&0&0&0&0&0&0&1&0&0&0&-1&0&0&0&0&0&0&0&0&0&0&0&0\\
0&0&0&0&0&0&0&0&0&0&0&0&0&0&0&0&0&0&0&0&0&0&0&0&0&0&0&0&0\\
2&0&2&0&2&0&2&0&2&0&2&0&2&0&0&0&-2&0&-2&0&-2&0&-2&0&-2&0&-2&0&-2\\
0&0&0&0&0&0&0&0&0&0&0&0&0&0&0&0&0&0&0&0&0&0&0&0&0&0&0&0&0\\
0&0&0&0&0&0&0&0&0&0&0&0&0&1&0&0&0&-1&0&0&0&0&0&0&0&0&0&0&0\\
0&0&0&0&0&0&0&0&0&0&0&0&0&0&0&0&0&0&0&0&0&0&0&0&0&0&0&0&0\\
0&0&0&0&0&0&0&0&0&0&0&1&0&0&0&0&0&0&-1&0&0&0&0&0&0&0&0&0&0\\
0&0&0&0&0&0&0&0&0&0&0&0&0&0&0&0&0&0&0&0&0&0&0&0&0&0&0&0&0\\
0&0&0&0&0&0&0&0&0&1&0&0&0&0&0&0&0&0&0&0&-1&0&0&0&0&0&0&0&0\\
0&0&0&0&0&0&0&0&0&0&0&0&0&0&0&0&0&0&0&0&0&0&0&0&0&0&0&0&0\\
0&0&0&0&0&0&0&1&0&0&0&0&0&0&0&0&0&0&0&0&0&0&-1&0&0&0&0&0&0\\
0&0&0&0&0&0&0&0&0&0&0&0&0&0&0&0&0&0&0&0&0&0&0&0&0&0&0&0&0\\
0&0&0&0&0&1&0&0&0&0&0&0&0&0&0&0&0&0&0&0&0&0&0&0&-1&0&0&0&0\\
0&0&0&0&0&0&0&0&0&0&0&0&0&0&0&0&0&0&0&0&0&0&0&0&0&0&0&0&0\\
0&0&0&1&0&0&0&0&0&0&0&0&0&0&0&0&0&0&0&0&0&0&0&0&0&0&-1&0&0\\
0&0&0&0&0&0&0&0&0&0&0&0&0&0&0&0&0&0&0&0&0&0&0&0&0&0&0&0&0\\
0&1&0&0&0&0&0&0&0&0&0&0&0&0&0&0&0&0&0&0&0&0&0&0&0&0&0&0&-1
\end{bmatrix} \quad (9)$$

The 3D plot and 2D contour plot of impulse response characteristic, $h(N,r,k)$, of the proposed 2D FIR filter from Eq. (4) for odd N=7, are given in the Fig. 3 and Fig. 4, respectively.

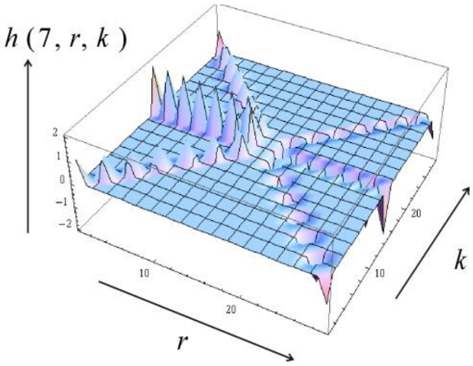

Fig. 3 3D plot of impulse response characteristic, $h(N,r,k)$, of the proposed 2D FIR filter from Eq. (4) for odd N =7

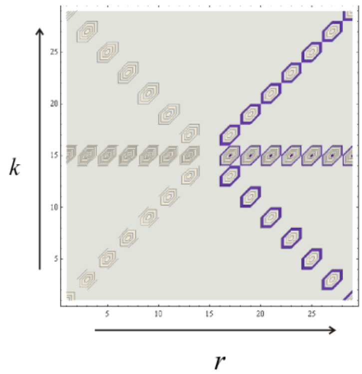

Fig. 4 2D contour plot of impulse response characteristic, $h(N,r,k)$, of the proposed 2D FIR filter from Eq. (4) for odd N =7

The 3D plot and 2D contour plot of impulse response characteristic, $h(N,r,k)$, of the proposed 2D FIR filter from Eq. (4) for even N=8, are given in the Fig. 5 and Fig. 6, respectively.

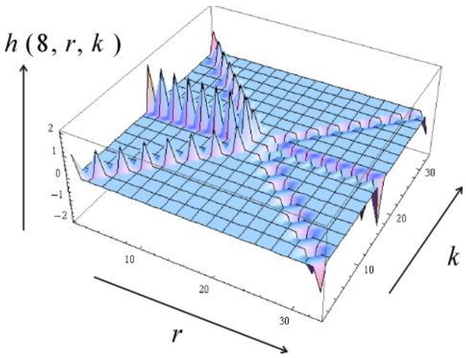

Fig. 5 3D plot of impulse response characteristic, $h(N,r,k)$, of the proposed 2D FIR filter from Eq. (4) for odd N =7

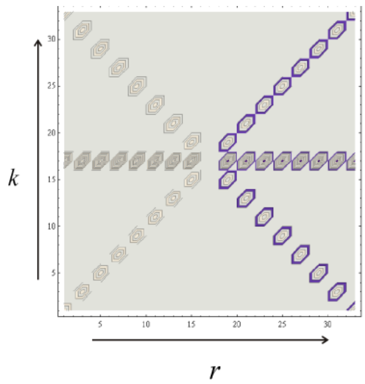

Fig. 6 2D contour plot of impulse response characteristic, $h(N,r,k)$, of the proposed 2D FIR filter from Eq. (4) for even N = 8

4. ANALYSIS OF THE MAGNITUDE AND PHASE CHARACTERISTICS OF PASS-BAND OF 2D FIR FILTER

We propose in previous research that the filter function, $H(N,z_1,z_2)$, is implemented as a product of three functions of successive orders $M-1$, M and $M+1$ and is given by the following expression

$$H(K,M,z_1,z_2)=[H(M-1,\ z_1,\ z_2)H(M,\ z_1,\ z_2)H(M+1,\ z_1,\ z_2)]^K \tag{10}$$

Amplitude response, $A(M,\ K,\ \omega_1,\ \omega_2)$, of the proposed filter function $H(K,M,\ z_1,\ z_2)$, has the form

$$\begin{aligned}A(M,K,\omega_1,\omega_2) = &\sum_{k=0}^{M-1}(\cos(2k\omega_1)+1)\sin(2k\omega_2)\cdot\\ &\cdot\sum_{r=0}^{M}(\cos(2r\omega_1)+1)\sin(2r\omega_2)\cdot\sum_{r=0}^{M}(\cos(2m\omega_1)+1)\sin(2m\omega_2)\end{aligned} \tag{11}$$

Magnitude characteristic is defined as

$$\left|H(M,\ K,\ e^{i\omega_1},\ e^{j\omega_2})\right| = \left|A(M,\ K,\ \omega_1,\ \omega_2)\right| \tag{12}$$

Liner-phase characteristic, $\varphi(M,K,\omega_1,\ \omega_2)$, of the proposed filter function $H(K,M,\ z_1,\ z_2)$, has the following form

$$\varphi(M,K,\omega_1,\omega_2) = -i\,K\,6\,N\,\omega_1) - j\,K(\frac{\pi}{2}+6\,N\,\omega_2) \tag{13}$$

Fig. 6 shows the phase characteristic of considered linear-phase multiplierless 2D FIR filter function in the initial part, for the same values of the free integer parameters K and M, i.e., $K = 3$ and $M = 7$.

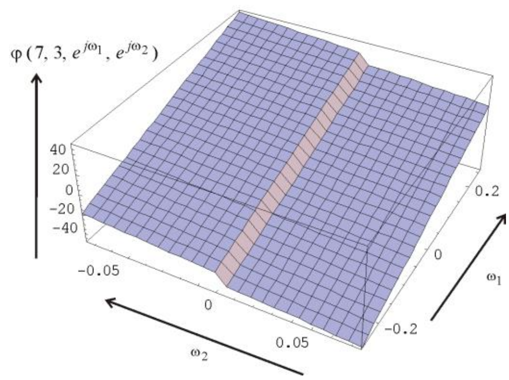

Fig. 6 3-D plot of the phase characteristic of proposed 2D FIR filter for $K = 3$ and $M = 7$

Using the standard technique, the amplitude, magnitude and phase characteristics are obtained from Eq. (5) for the numerical values $K = 3$ and $M = 7$, and detailed characteristics of the filter function, $H(K,M,z_1,z_2)$, are given in the following figures.

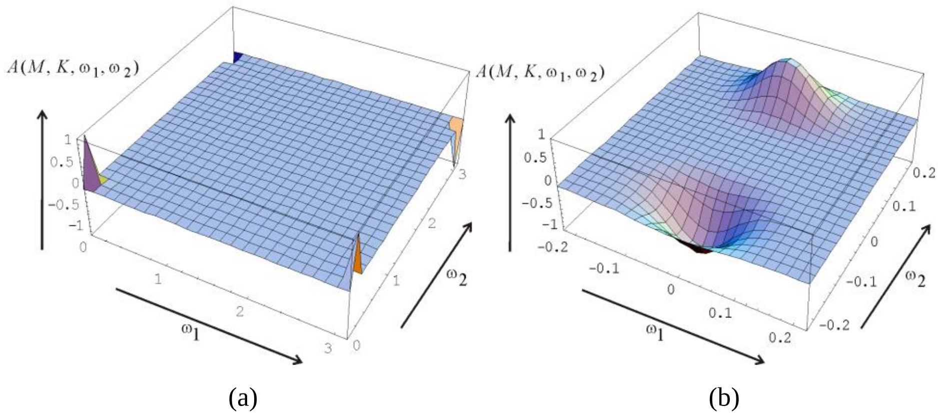

Fig. 7 a) 3D plot of normalized amplitude characteristics of the proposed 2D FIR filter for K=3 and M=7; b) Zoomed panel

Illustrated examples of pass-band characteristics of the considered FIR filter function for given values of attenuation, $a(K, M, \omega_1, \omega_2)$, are shown in Fig. 8-9.

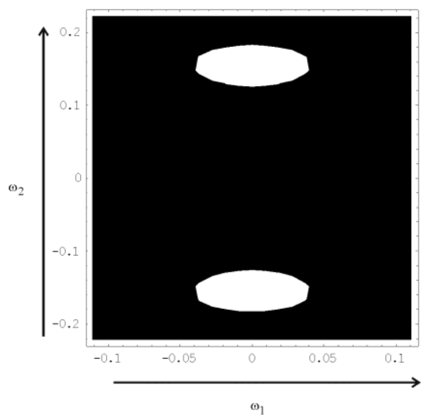

Fig. 8 2D contour plot of normalized magnitude characteristics, shape of the pass-band with attenuation of 3 dB for K=3 and M=7, zoomed

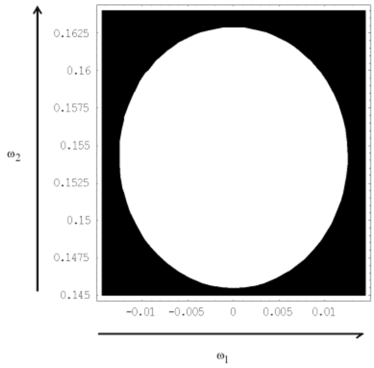

Fig. 9 2D contour plot of normalized magnitude characteristics - shape of the pass-band with attenuation of 0.28 dB for *K*=3 and *M*=7

In Table 1 are given the values of the surface area of pass-band of considered 2D FIR filter function for different values of given maximal attenuation. Results are given in (%) in relation to a total area of the amplitude characteristic.

Table 1 Normalized surface area of pass-band for proposed 2D FIR filter function for given values of maximal attenuation

K	*M*	a_{pass} (dB)	Normalized surface area of the filter function pass-band
3	7	0.28	$3.4578915556\ 10^{-5}$
3	7	3	$3.7150111987\ 10^{-4}$

5. Analysis of the Magnitude Characteristics of Pass-Band and Stop-Band of 2D FIR Filter

In Table 2 are given the values of the surface area of stop-band of considered 2D FIR filter function for different values of given minimal attenuation in relation to a total area of the amplitude characteristic.

Table 2 Normalized surface area of stop-band for 2D FIR filter function for given values of minimal attenuation

K	*M*	a_{stop} (dB)	Normalized surface area of the filter function stop-band (%)
3	7	140	64.6703039362
3	7	120	71.3833333333
3	7	100	80.3949427005
3	7	80	84.9030144494
3	7	60	92.3301195815
3	7	40	97.7362232187

For given values of free integer parameters M=7 and K=3, an example of characteristics shapes of stop-band of considered 2D FIR filter function for a set of values of attenuation $a(M, K, \omega_1, \omega_2)$ = [160*dB*, 140*dB*, 120*dB*, 100*dB*, 80*dB*, 60*dB*] is shown in Fig. 10.

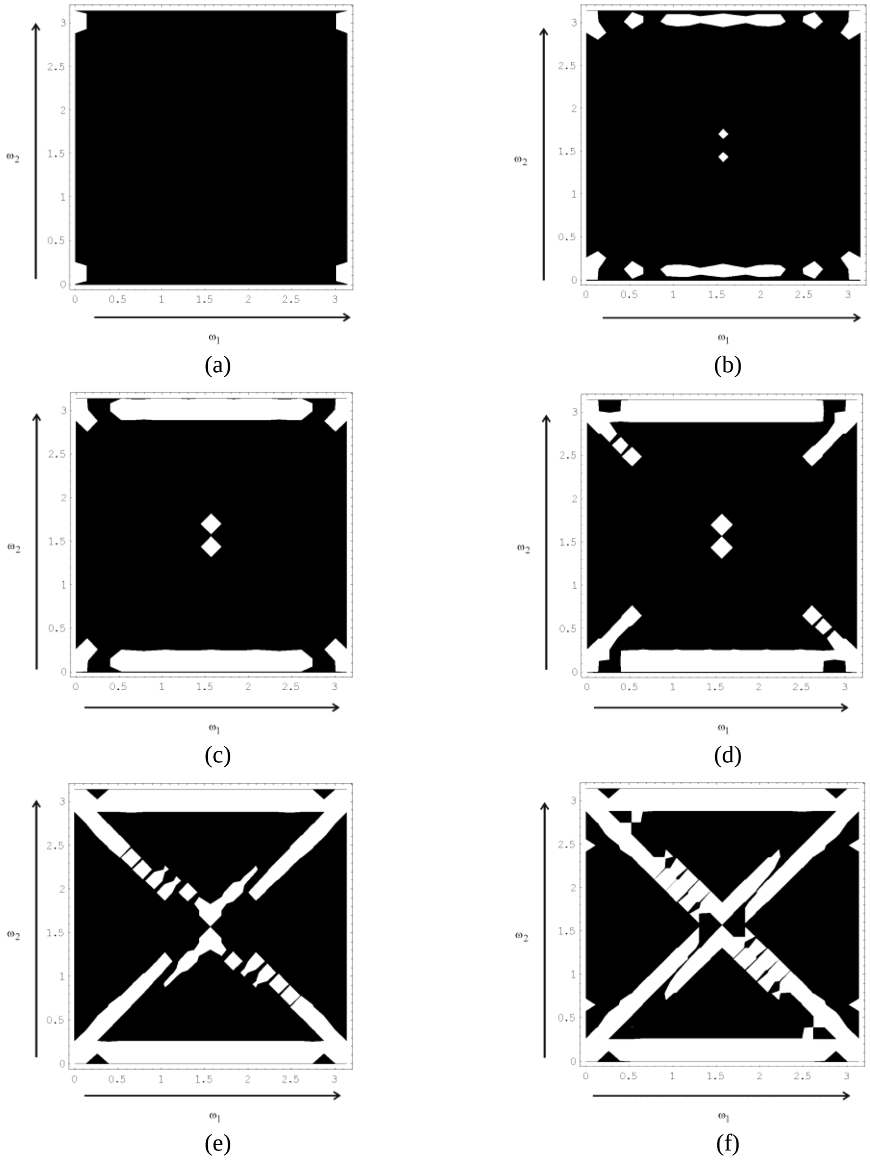

Fig. 10 2D contour plot of normalized magnitude characteristics of 2D FIR filter function for M=7 and K=3. (a) Shape of the stop-band with attenuation of 40 dB. (b) Shape of the stop-band with attenuation of 60 dB. (c) Shape of the stop-band with attenuation of 80 dB. (d) Shape of the stop-band with attenuation of 100 dB. (e) Shape of the stop-band with attenuation of 120 dB. (f) Shape of the stop-band with attenuation of 140 dB.

6. Conclusion

This paper presents an original approach to the multiplierless linear-phase spike 2D symmetric FIR digital filter function synthesis, bringing the significant improvements in the filter theory. The new modified 2D Christoffel-Darboux formula for continuous classical orthogonal Chebyshev polynomials of the first and classical orthogonal Chebyshev polynomials of the second kind is proposed in this paper, by new analytical method, in a compact explicit form.

The impulse response coefficients of proposed 2D FIR filter functions are presented in this paper, and corresponding examples of impulse response are illustrated.

Elegant explicit transition from the continuous domain into 2D z domain without residuum and without errors is successfully demonstrated. This new formula can be directly applied in generating selective spike 2D FIR filter functions. All parasitic effects, Gibbs's phenomenon, are suppressed and there is no need for using of multipliers.

Filters design by the proposed method can be applied in various areas, such as telecommunications, medicine, pharmacy, seismology, general localizations and diagnostics where they can be of special interest.

The illustrated examples of the three-dimensional frequency responses and corresponding 2D contour plots of proposed linear-phase symmetric 2D FIR filter are also presented. These examples illustrate the high advantages of the proposed approach and efficient way of designing high selective filters.

The paper presents a detailed analysis of size of the surface area of pass-band and a set of values of surface area of stop-band of multiplierless linear-phase 2D FIR filter function described in in previous research. Explicitly are given the sizes of characteristic bands of filter function for given values of attenuation.

Normalized surface area of the filter function pass-band with diamond sharpness spike multiplierless linear-phase 2D FIR filter is 3.4578915556 10^{-5} with maximal attenuation of 0.28 *dB*. Normalized surface area of the filter function stop-band is 80.395% for the given minimal attenuation of 100 dB.

References

[1] G. Szegö, *Orthogonal polynomials* New York: American Mathematical Society, Colloquium Publications, 1967, vol. 23.

[2] M. Abramowitz, I. Stegun, *Handbook on mathematical function*. National Bureau of Standards, Applied Mathematics Series, USA, 1964.

[3] V. D. Pavlović, "New Class of Filter Functions generated directly by the modified Christoffel–Darboux formula for classical orthonormal Jacobi polynomials", *International Journal of Circuit Theory and Applications – John Wiley & Sons*, vol. 40, pp. 1–15, 2012. (to be published, DOI: 10.1002/cta.1817)

[4] V. D. Pavlović, A. D. Ilić, "New class of filter functions generated most directly by Christoffel–Darboux formula for classical orthonormal Jacobi polynomials", *International Journal of Electronics–Taylor & Francis*, vol. 98, No. 12, pp. 1603–1624, 2011.

[5] A. D. Ilić, V. D. Pavlović, "New class of filter functions generated most directly by Christoffel–Darboux formula for Gegenbauer orthogonal polynomials", *International Journal of Electronics–Taylor & Francis*, vol. 98, No. 1, pp. 61–79, 2011.

[6] J. R. Djordjevic-Kozarov, V. D. Pavlovic, " An Analytical Method for the Multiplierless 2D FIR Filter Functions and Hilbert Transform in z2 domain", *IEEE Transactions on Circuits and Systems- II:Express briefs*, vol. 60, no. 8, 2013. DOI: 10.1109/TCSII.2013.2268340

[7] V. D. Pavlović, N. Doncov, D. G. Ćirić, "1D and 2D Economical FIR Filters Generated by Chebyshev Polynomials of the First Kind", *International Journal of Electronics. – Taylor & Francis*, vol. 100, no. 11, pp. 1592-1619, 2013.

[8] S. Lj. Peric, D. S. Antic, V. D. Pavlovic, S. S. Nikolic, and M. T. Milojkovic, "Ultra-selective lowpass linear-phase FIR filter function", *IET Electronics Letters*, vol. 49, no. 9, pp. 595-597, 2013.

[9] S. C. Dutta Roy, "Impulse response of sincN FIR filters", *IEEE Transactions on Circuits and Systems*, vol. 53, No. 3, pp. 217–219, 2006.

[10] A. Fernandez-Vazquez, and G. Jovanovic-Dolecek, "Maximally Flat CIC Compensation Filter: Design and Multiplierless Implementation", ", *IEEE Transactions on Circuits and Systems- II:Express briefs,* Vol. 59, No. 2, pp. 113-117, 2012.

[11] J. O. Coleman, "Chebyshev Stopbands for CIC Decimation Filters and CIC-Implemented Array Tapers in 1D and 2D", *IEEE Transactions on Circuits and Systems- I: Regular Paper,* Vol. 59, No. 12, pp. 2956-2968, 2012.

[12] S. N. Hazra and M. S. Reddy, "Design of circularly symmetric low-pass two-dimensional FIR digital filters using transformation", IEEE Trans. Circuits Syst., vol. CAS-33, no. 10, pp. 1022–1026, Oct. 1986.

[13] R. H. Yang and Y. C. Lim, "Grid density for design of one- and two-dimensional FIR filters,"Electron. Lett., vol. 27, no. 22, pp. 2053–2055, Oct. 1991.

[14] S. H. Low and Y. C. Lim, "Frequency grid density for the design of 2-D FIR filters,"Electron. Lett., vol. 32, no. 16, pp. 1460–1461, Aug. 1996.

[15] A. Klouche-Djedid and S. S. Lawson, "Simple design and realisation of linear phase 2D FIR filters with diamond frequency support," Electron. Lett., vol. 35, no. 14, pp. 1148–1150, Jul. 1999.

[16] N. Vijayakumar and K. M. M. Prabhu, "Two-dimensional FIR compaction filter design,"Proc. Inst. Elect. Eng.—Vis. Image Process., vol. 148, no. 3, pp. 173–181, Jun. 2001.

[17] V. L. Narayana Murthy and A. Makur, "Design of some 2-D filters through the transformation technique," Proc. Inst. Elect. Eng.—Vis. Image Pro-cess., vol. 143, no. 3, pp. 184–190, Jun. 1996.

[18] A. Anvari Moghaddam and A. R. Seifi, "Study of forecasting renewable energies in smart grids using linear predictive filters and neural networks", IET Renew. Power Gen., vol. 5, no. 6, pp. 470–480, Nov. 2011.

[19] X. Lai and Y. Cheng, "A sequential constrained least-square approach to minimax design of 2-D FIR filters,"IEEE Trans. Circuits Syst. II, Exp. Briefs, vol. 54, no. 11, pp. 994–998, Nov. 2007.

[20] J. C. Liu and Y. L. Tai, "Design of 2-D wideband circularly symmetric FIR filters by multiplierless high-order transformation,"IEEE Trans. Circuits Syst. I, Reg. Papers, vol. 58, no. 4, pp. 746–754, Apr. 2011.

[21] S. K. Mitra, Digital Signal Processing. New York, NY, USA: McGraw–Hill, 1998.